Electronic Supplementary Information

for

Redox Preparation of Mixed-valence Cobalt Manganese Oxide Nanostructured Materials: Highly Efficient Noble Metal-free Electrocatalysts for Sensing Hydrogen Peroxide

By Cheng-Chi Kuo, Wen-Jie Lan and Chun-Hu Chen*

Department of Chemistry, National Sun Yat-sen University, Kaohsiung, Taiwan 80424

Figure S-1: The XRD patterns of the SCM precursors before calcination at 500°C. (A) The patterns of the **SCM-100** precursor prepared at 100°C, showing a single phase corresponding to CoOOH-like structure (JCPDS-07-169). (B) The patterns of the **SCM-200** precursors prepared at 200°C. More than one phase was shown in the sample. In addition to the CoOOH-like structure, reflections labeled by the start marks correspond to a γ-MnO_2 Phase.[1]

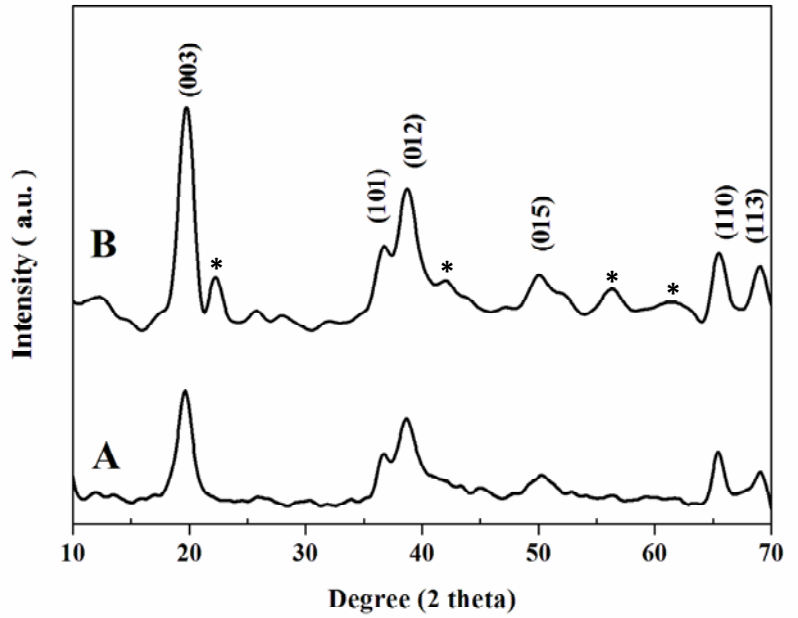

Figure S-2. The XPS spectra of Co 2p and Mn 2p in the calcined SCM products and uncalcined hydroxide precursors. (a) The binding energy (BE) values of Co $2p_{3/2}$, Co $2p_{1/2}$, and the satellite peak in the uncalcined precursors are 781.1, 796.2, and 790.8 eV, respectively, corresponding to Co(III).[2] In SCM products, the BE of Co $2p_{3/2}$ and Co $2p_{1/2}$ are 779.8 and 795.0 eV, respectively. Together with the absence of satellite peak at 790.8 eV, the spectra of SCM show a good agreement with the mixed valence of Co(II) and Co(III) in spinel Co_3O_4.[3, 4] (b) The Mn species in the uncalcined precursors show Mn $2p_{3/2}$ and Mn $2p_{1/2}$ with values of 642.5 and 654.2 eV, respectively. These values correspond well to the Mn (IV) in the literature.[5] The Mn spectra of SCM products after calcination are similar to these of the uncalcined precursors, showing the difficulty to determine the mixed-valence systems of manganese due to the line-broadening effect.[6]

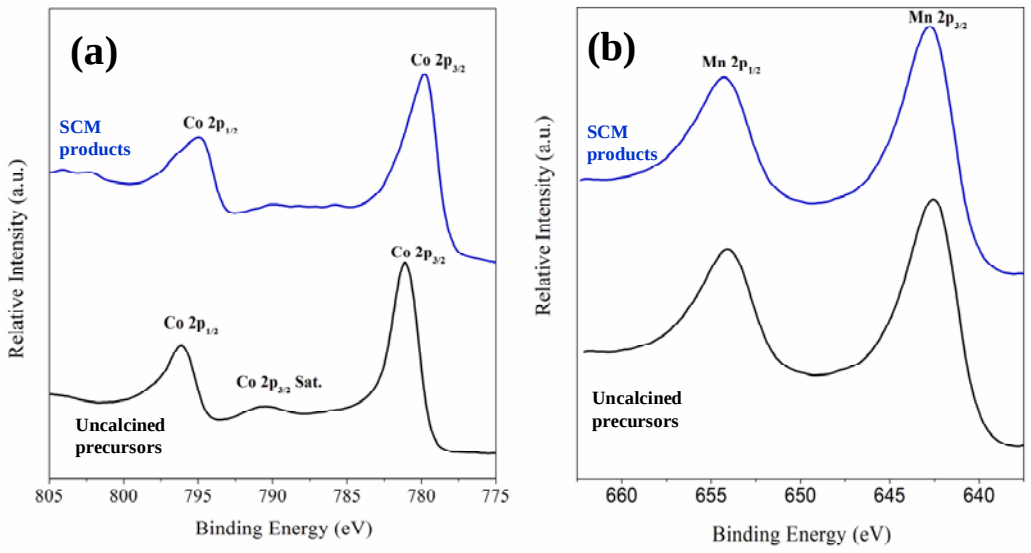

Figure S-3. The SEM images of the SCM samples prepared at different temperatures: (a) 60°C, (b) 80°C, (c) 150°C, and (d) 200°C. The SEM results show that the 3D nanostructures in the samples prepared at 60°C (**SCM-60)** are not completely developed. However, the interconnection network features, plausibly to be the "seeds" of nanoflakes, were already observed on the surface. The samples generated at 80°C (**SCM-80**) are starting to form the flower-like nanostructures. The surface of nanoflakes in the samples produced at 150°C (**SCM-150)** was further expanded, leading to the size enlargement of the voids surrounded by the expanded nanoflakes. With the increase of reaction temperatures to 200°C (**SCM-200**), additional nanowire features were observed with the presence of nanoflaked microspheres together (Fig. S-2d). The white and yellow arrows in (d) indicate the presence of nanoflakes and nanowires, respectively.

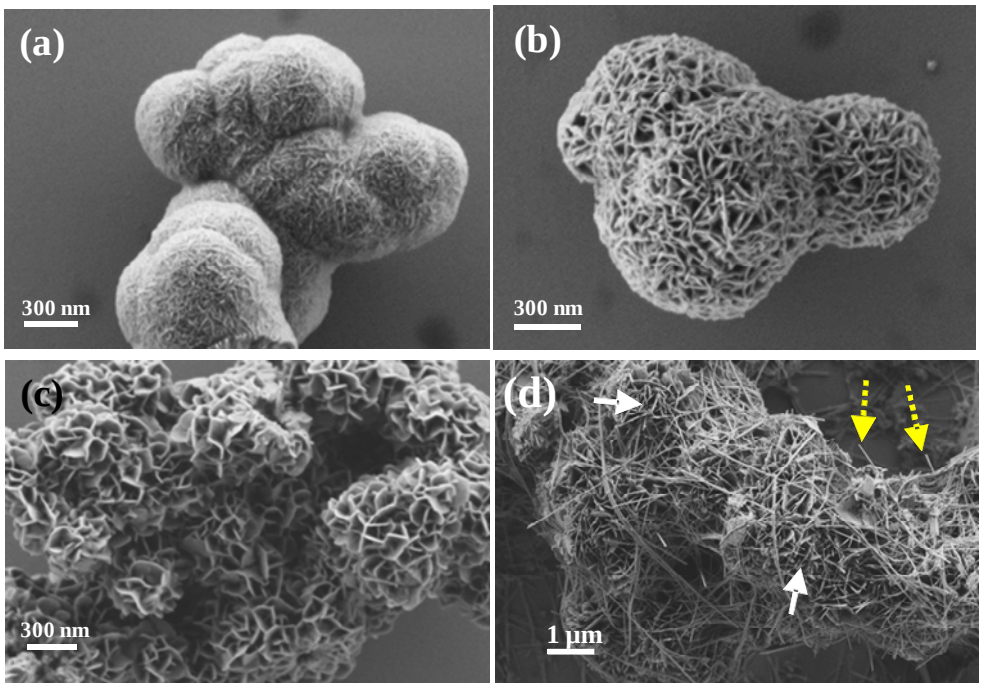

Figure S-4. The pore size distribution comparison of (a) **SCM-100** and (b) **SCM-150**.

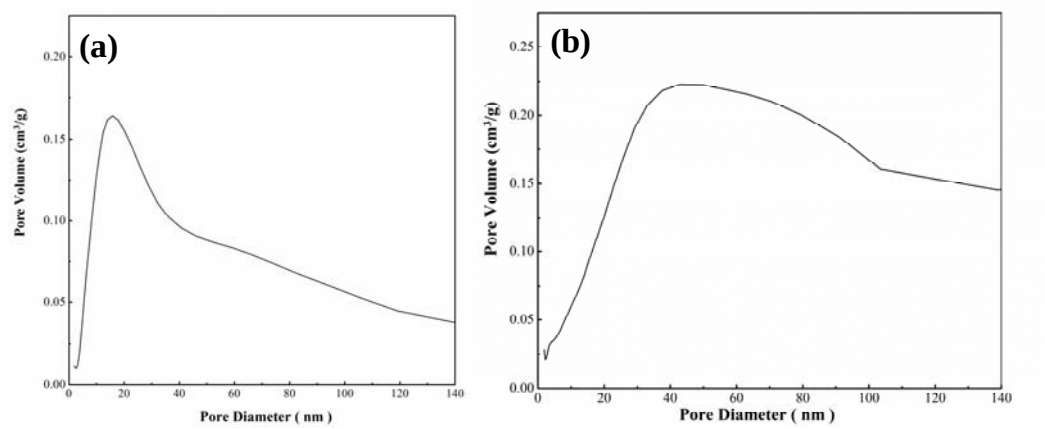

Figure S-5. The baseline stabilization of **SCM-100** before performing H_2O_2 measurement. The required stabilization time is less than 10 seconds.

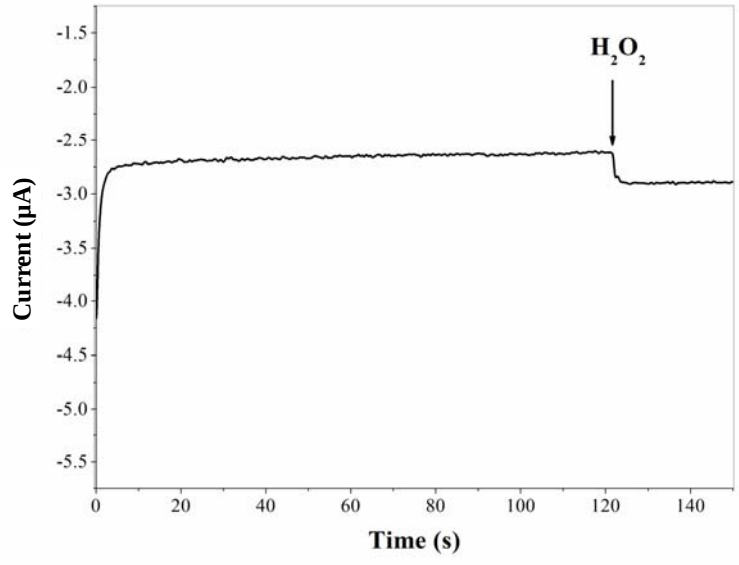

Figure S-6. The sensitivity comparison of **SCM-100** and commercial-available Co_3O_4 materials.

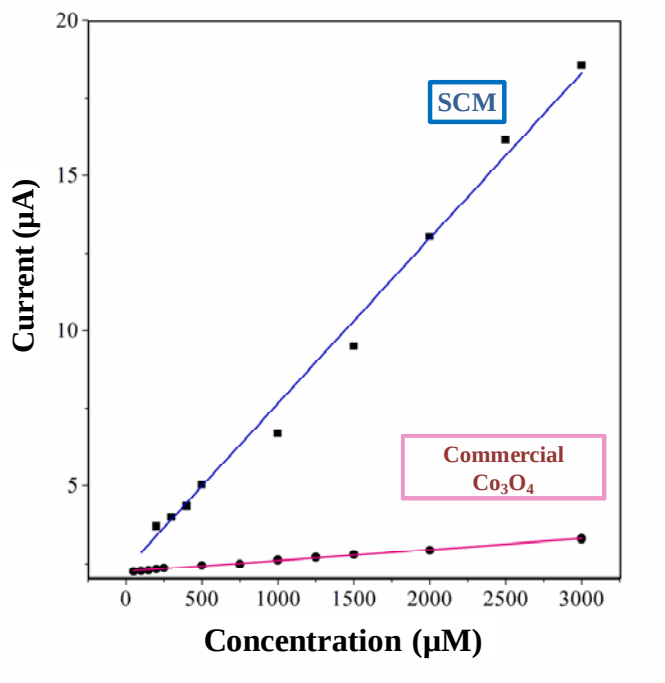

Figure S-7. The amperometric current responses of **SCM-100** at -0.65 V towards 1 mM H_2O_2 in PBS solution (a), and the long-term stability of continuous H_2O_2 sensing for 7 days (b).

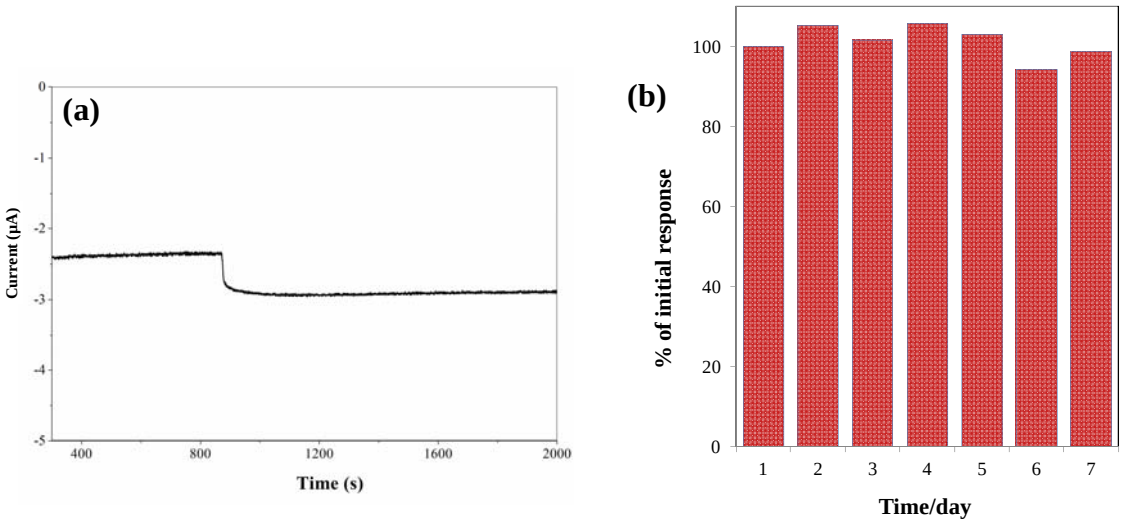

Figure S-8. The CV results of different electrocatalysts in PBS with the presence of 1 mM H_2O_2: bare GCE (red dot-dash line), commercial Co_3O_4 (black dash line) and **SCM-100** (blue solid line). The H_2O_2 oxidation signals above 0.80 V of **SCM-100** and commercial Co_3O_4 were similar to each other.

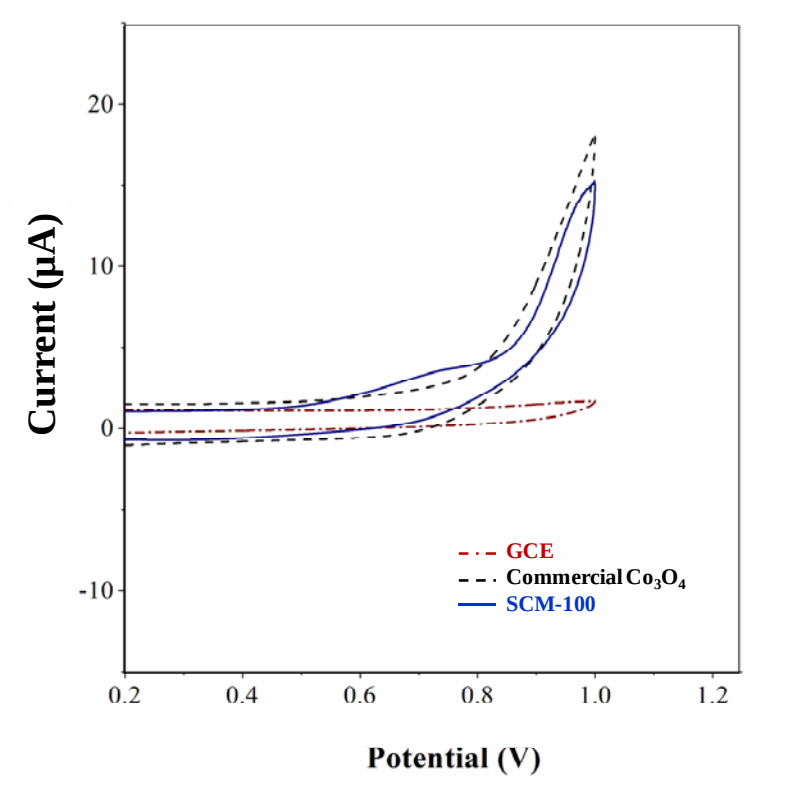

Figure S-9. The SEM studies of formation processes in **SCM-200**. (a) The bulk MnO_2 nanowire bundles. The inset of EDXS results shows that the manganese is the majority in the nanowire bundles with a small amount of cobalt. (b), (c) The formation of nanoflakes (white solid-line arrows) was observed on both the terminals and centers of bulk MnO_2 nanowire bundles, respectively. The yellow dash-line arrows indicate the separated nanowires in MnO_2 bulk bundles. The red box in (c) shows the growth interfaces of MnO_2 bundles and SCM nanoflakes. (d) The completed separation of nanowires from the bundles (yellow dash-line arrows), and their wrapping/covering on the SCM microspheres (white solid-line arrows) were observed. This image is identical to that in Fig. S-3d.

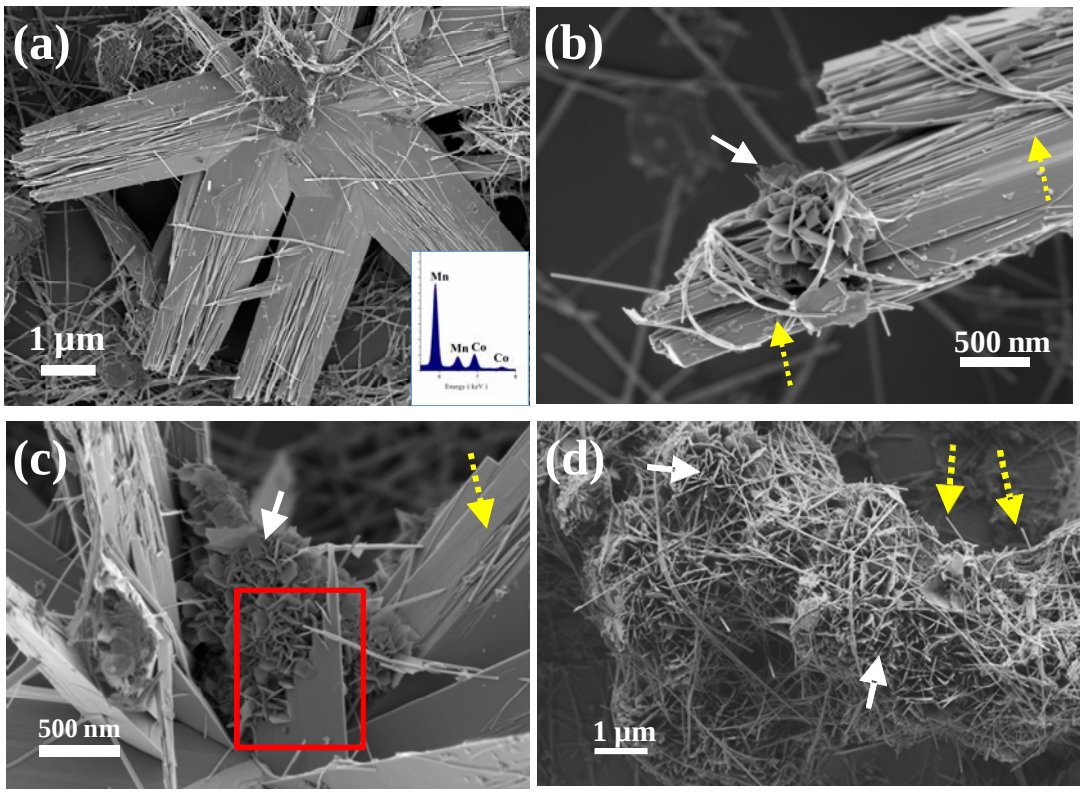

Table S-1. The comparison of electrochemical sensing of H_2O_2 with noble metal materials

Electrode Materials	Electrolyte	Applied Potentials (V vs. Ag/AgCl)	Linear Range (mM)	Sensitivity	Detection limit (μM)	Ref
Au Nanoplates	0.2M PBS pH 6.5	-0.3	0.1-50	N.A.	4	[7]
SiO_2@Au	0.1M PBS pH 6.5	-0.4	0.005-1	N.A.	2	[8]
Porous Au-Pt NPs Electrode	PBS pH=7.4	0.4	0.01-3	381.8 (μA/mM-cm^2)	10	[9]
Roughed Ag Electrode	0.2M PBS pH=7.0	-0.3	0.01-22.5	N.A.	6	[10]
Au NPs/MWCNT/PANI/ Au	0.1M PBS pH=7.0	0.6	0.003-0.6	3.3 (μA/mM)	0.3	[11]
Ag NP/TiO_2 NW	0.2M PBS (pH=7.4)	-0.3	0.1-60	N.A.	1.7	[12]
Spinel Cobalt manganese oxides (**SCM-100**)	0.1M PBS (pH = 7.4)	-0.65	0.1-25	2.9 (μA/mM)	15	This work

Table S-2. The comparison of electrochemical sensing of H_2O_2 with metal oxide related materials

Electrode Materials	Electrolyte	Applied Potentials (V vs. Ag/AgCl)	Linear Range (mM)	Sensitivity	Detection limit (μM)	Ref
rGO-Fe_3O_4	PBS pH 7.0	-0.3	0.1-6	688 (μA/mM-cm^2)	3.2	[13]
MnO_x	0.1M PBS pH 7.0	-0.4	0.02-1.26	2.72 (μA/mM)	20	[14]
CuO	0.1M NaOH	-0.25	0.1-36	N.A.	2	[15]
CoOOH	0.1M NaOH	0.1	0.01-1.2	79 (μA/mM)	40	[16]
Cu_2S	0.1M PBS pH 7.4	-0.35	0.01-3.75	N.A.	1.1	[17]
Co_3O_4	0.05M PBS pH 7.4	-0.77	0-1.7	N.A.	N.A.	[18]
AgNP/F-SiO_2/GO	0.2M PBS pH 6.5	-0.3	0.1-260	N.A.	4	[19]
Spinel Cobalt manganese oxides (**SCM-100**)	0.1M PBS (pH = 7.4)	-0.65	0.1-25	2.9 (μA/mM)	15	This work

Table S-3. The elemental analyses of a series of cobalt manganese oxide materials

Initial Co:Mn ratios[a]	Co/Mn ratios of the hydroxide precursors[b]		Co/Mn ratios of the SCM products	
	ICP-MS	EDXS	ICP-MS	EDXS
3:1	2.39	2.33	-	-
4:1	2.66	2.68	2.71	2.62
6:1	2.78	2.74	-	-
10:1	2.99	2.95	-	-

[a]The mole ratios of Co:Mn in the initial preparation mixtures

[b]The data were adopted from Ref. 2

Reference

1. L. Jin, L. Xu, C. Morein, C.-H. Chen, M. Lai, S. Dharmarathna, A. Dobley and S. L. Suib, *Adv. Funct. Mater.*, 2010, **20**, 3373-3382.
2. W.-J. Lan, C.-C. Kuo and C.-H. Chen, *Chem. Commun.*, 2013, **49**, 3025-3027.
3. Z.-Y. Tian, P. H. Tchoua Ngamou, V. Vannier, K. Kohse-Höinghaus and N. Bahlawane, *Appl. Catal., B*, 2012, **117-118**, 125-134.
4. J. C. Carver and G. K. Schweitzer, *J. Chem. Phys.*, 1972, **57**, 973.
5. X.-S. Liu, Z.-N. Jin, J.-Q. Lu, X.-X. Wang and M.-F. Luo, *Chem. Eng. J.*, 2010, **162**, 151-157.
6. E. C. Njagi, C.-H. Chen, H. Genuino, H. Galindo, H. Huang and S. L. Suib, *Appl. Catal., B*, 2010, **99**, 103-110.
7. R. Ning, W. Lu, Y. Zhang, X. Qin, Y. Luo, J. Hu, A. M. Asiri, A. O. Al-Youbi and X. Sun, *Electrochim. Acta*, 2012, **60**, 13-16.
8. J. Shen, X. Yang, Y. Zhu, H. Kang, H. Cao and C. Li, *Biosens. Bioelectron.*, 2012, **34**, 132-136.
9. Y. J. Lee, C. Oh, J. Y. Park and Y. Kim, *IEEE Trans. Nanotechnol.*, 2011, **10**, 1298-1305.
10. W. Lian, L. Wang, Y. Song, H. Yuan, S. Zhao, P. Li and L. Chen, *Electrochim. Acta*, 2009, **54**, 4334-4339.
11. J. Narang, N. Chauhan and C. S. Pundir, *Analyst*, 2011, **136**, 4460-4466.
12. X. Qin, W. Lu, Y. Luo, G. Chang, A. M. Asiri, A. O. Al-Youbi and X. Sun, *Electrochim. Acta*, 2012, **74**, 275-279.
13. Y. Ye, T. Kong, X. Yu, Y. Wu, K. Zhang and X. Wang, *Talanta*, 2012, **89**, 417-421.
14. S. Thiagarajan, T. H. Tsai and S.-M. Chen, *Int. J. Electrochem. Sci.*, 2011, **6**, 2235-2245.
15. M. U. Prathap, B. Kaur and R. Srivastava, *J. Colloid Interface Sci.*, 2012, **370**, 144-154.
16. K. K. Lee, P. Y. Loh, C. H. Sow and W. S. Chin, *Biosens. Bioelectron.*, 2013, **39**, 255-260.
17. S. K. Maji, A. K. Dutta, G. R. Bhadu, P. Paul, A. Mondal and B. Adhikary, *J. Mater. Chem. B*, 2013, **1**, 4127.
18. H. Pang, F. Gao, Q. Chen, R. Liu and Q. Lu, *Dalton Trans.*, 2012, **41**, 5862-5868.
19. W. Lu, Y. Luo, G. Chang and X. Sun, *Biosens. Bioelectron.*, 2011, **26**, 4791-4797.